

Coherent versus Incoherent Energy Transfer and Trapping in Photosynthetic Antenna Complexes

Jan A. Leegwater

Department of Physics and Astronomy, Vrije Universiteit Amsterdam, De Boelelaan 1081,
1081 HV-NL Amsterdam, The Netherlands

Received: May 17, 1996[®]

In this paper we present a study of a model in which there is energy transfer as well as a special site where an irreversible reaction takes place. This model has an arbitrary ratio of homogeneous broadening versus site interaction energy. This allows us to study the crossover from hopping dynamics to exciton dynamics. We show that for the survival time the hopping (Förster) approximation gives a surprisingly accurate final result even when the energy transfer is excitonic. Fluorescence depolarization however is a sensitive probe for the nature of the energy transfer. We study the number of coherent molecules by considering a generalization of the inverse participation ratio. For LH1, assuming that it is a ring of 16 dimers, we estimate that the excitation is, on the average, delocalized over two dimers. The excitation is localized by phonons.

I. Introduction

In the photosynthetic light-harvesting complex excitation energy is transferred between antenna pigments and eventually from antenna pigments to the photosynthetic reaction center. It is often assumed that this energy transfer takes place through the Förster mechanism.¹ In the Förster picture at all times a specific molecule is excited, and the excitation hops from one molecule to the next as a result of the dipole–dipole interaction. There are well-known antenna system for which the Förster picture is expected to be invalid. For instance in the so-called FMO complex² the pigments are so close together that, on the basis of arguments presented in this paper, the excitation must be considered to be delocalized over a number of pigments, and the excitation dynamics cannot be described at all by the Förster mechanism.

To advance the discussion of the coherence of the excitations, we study here a model in which the limiting cases of Förster transfer and completely delocalized excitonic states are continuously connected to each other. The most important parameter determining this crossover is the interaction energy J divided by the homogeneous line width Γ . Because of the continuous connection of the limiting cases, the issues involved in exciton coherence versus Förster incoherence can be discussed in a clean way. In this paper the homogeneous line width is primarily caused by fluctuations in the transition frequency due to phonons. In a spectroscopic language what we call homogeneous line width corresponds to T^* processes. The motivation for denoting these processes as homogeneous is that the dephasing process is assumed to be fast.³ This is to be contrasted with inhomogeneous broadening, which is caused by static disorder that has to be taken into account by averaging the final quantities under consideration.

In biophysical systems, a typical interaction is that of two bacteriochlorophyll molecules located at a distance of about $r = 1$ nm.⁴ As the transition dipole transition moment is on the order of $\mu = 7$ D, the interaction strength can be $J = \mu^2/r^3 \approx 250$ cm⁻¹. However, in Δ OD spectra frequently features are noticeable that are separated by 10 nm at a wavelength of 850 nm. This corresponds to an energy on the order of 120 cm⁻¹. We can obtain an estimate of the homogeneous line width Γ

by identifying it with the smallest energy on which features are noticeable. So an estimate for the Förster limit parameter $J/\Gamma = 2$. This parameter may be larger for certain systems, as also inhomogeneous broadening can be important. An estimate for the amount of inhomogeneous broadening is 200 cm⁻¹, so that it is of magnitude similar to the homogeneous line width. The estimate given here is compatible with other estimates for C-phycocyanin,⁵ allophycocyanin,⁶ and photosystem II.⁷ Clearly, on the basis of these estimates the study of exciton coherence in photosynthetic antenna systems is highly relevant. We should point out that the model studied here has been extensively studied in a condensed matter physics context.⁸ In these studies the emphasis was on the derivation and on the validity of the resulting dynamic equations. Here we provide explicit solutions of the resulting equations, and we put the emphasis on the properties of this solution.

This paper is organized as follows. In section II we describe the model of the antenna system and demonstrate the Green function solution. In section III it is shown that in the limit of large inhomogeneously broadened lines Förster transfer is recovered. In section IV we present numerical results for a ring of pigments and show that as far as the excitation lifetime goes, the Förster hopping picture gives a good approximation. In section V we show that fluorescence depolarization is sensitive to the mode of energy transfer and that a consistent interpretation in terms of Förster transfer in general is not possible. Finally in the Discussion, section VI, we present a generalization of the well-known inverse participation ratio and argue that it is a good measure of the average number of coherently excited molecules.

II. Model Hamiltonian

We consider a Frenkel exciton model where the various pigments are coupled to each other by interactions J . Typically we will consider dipole–dipole or nearest neighbor interactions, but for the moment we will use a general interaction. The (tight binding) Hamiltonian is

$$H_0 = \sum_i \hbar \omega_i |i\rangle\langle i| + \frac{1}{2} \sum_{i \neq j} J_{ij} (|i\rangle\langle j| + |j\rangle\langle i|) \quad (1)$$

where $|i\rangle$ and $|j\rangle$ denote electronic states in which molecule i

[®] Abstract published in *Advance ACS Abstracts*, August 1, 1996.

(or j) is excited. The first term in H_0 describes the transition energies of the molecules. We have allowed for the sites to have different excitation energies ω_i . Inhomogeneous broadening is described by taking the transition frequencies to be random variables taken from some (usually Gaussian) distribution. The second term on the right-hand side in eq 1 is the interaction term. One of the consequences of this interaction is that an excitation can be transferred from a molecule i to another molecule j .

We assume that there is also homogeneous broadening in the model, due to phonons. For simplicity we will assume that each molecule has its own heat bath, which is correct when there is no phonon-mediated interaction between molecules. The phonons cause a time dependent shift of the isolated molecule transition frequency, but the phonons do not give rise to a decrease of the number of excited molecules. This is effected by adding an exciton–phonon interaction term V to the Hamiltonian

$$V = \sum_{k_i} C_{i,k_i} |i\rangle\langle i| (B_{i,k_i}^\dagger + B_{i,k_i}) \quad (2)$$

where B^\dagger and B are creation and annihilation operators for the phonons, and the phonon Hamiltonian is

$$H_{\text{ph}} = \sum_{k_i} \Omega_{k_i} B_{i,k_i}^\dagger B_{i,k_i} \quad (3)$$

Note that the interaction operator V commutes with the operator counting the number of excited molecules $\sum_i |i\rangle\langle i|$. Equation 2 can be made plausible as follows: Any time a phonon comes along, the operator B^\dagger or B has a certain expectation value. Then the isolated molecule transition frequency ω_i is modified by an amount proportional to C_{i,k_i} . We have not included the dependence of the interaction energy J_{ij} on the intermolecular distance in the coupling with the phonons. We expect that this off-diagonal dependence is much smaller than diagonal exciton–phonon coupling simply because the energies involved differ by almost 2 orders of magnitude. Below we will average over the phonon degrees of freedom.

We further include a special molecule in the model on which an excitation can decay irreversibly. This special molecule can model the reaction center of the antenna complex or, as is done in section V, a singlet–singlet annihilation site. This irreversible decay can be described in many ways. The most convenient way is to add a non-hermitian term to the Hamiltonian,

$$H_i = -i \frac{\Gamma_d}{2} |1\rangle\langle 1| \quad (4)$$

so that the total, non-hermitian Hamiltonian is given by

$$H_T = H + V + H_{\text{ph}} \quad (5)$$

with the phonon independent part

$$H = H_0 + H_i \quad (6)$$

The phonons give rise to loss of phase coherence. To describe this properly, we must use the reduced density matrix $\rho(t)$. The density matrix is the average of the state $|\psi, k_i\rangle$ over the phonon degrees of freedom,

$$\rho(t) = \text{Tr}_{\{k_i\}} |\psi, k_i\rangle\langle\psi, k_i| \quad (7)$$

Here ψ refers to the system part of the wave function, and k_i to the phonon part. There are two classes of matrix elements in

the density matrix. The diagonal elements $\rho_{i,i}$ are the probabilities of finding molecule i in the excited state. The off-diagonal elements $\rho_{i \neq j}$ describe the coherence between molecules i and j . The phase coherence between molecules i and j decays when a phonon is absorbed or emitted by molecule i since then the transition frequency is changed, and as a result, the phase is changed by some random amount.

The temperature of the systems enters through the probability distribution of the phonons at time $t = 0$. We will consider the limit in which the phonon correlation time is much shorter than other times so that it can be approximated by a δ function. While the phonon correlation time is not really known, it is quite possible that it is on the order of 50 fs. Thus, the phonon correlation time may be important for ultrafast experiments. This, however, is beyond the scope of this paper. Due to the quantum fluctuation dissipation theorem,³ a zero correlation time can only occur at high temperatures. This is the motivation for limiting ourselves to the high-temperature situation in this paper. After taking the average over the phonon degrees of freedom, the time evolution of the density matrix is given by^{8–10}

$$\frac{d}{dt} \rho(t) = -iH\rho(t) + i\rho(t)H^* - \hat{\Gamma}'\rho(t) \quad (8)$$

where the asterisk denotes complex conjugation. This careful treatment of the complex conjugation is needed to correctly describe the irreversible decay. The operator Γ' describes the loss of phase coherence due to the interaction with phonons. It is all that remains of the phonons after the average over the phonon degrees of freedom has been taken. In the site basis set the action of Γ' is given by

$$\hat{\Gamma}'|i\rangle\langle j| = \Gamma(1 - \delta_{ij})|i\rangle\langle j| \quad (9)$$

where Γ is a number that corresponds to the homogeneous line width. Fluctuations in frequency due to the phonons give rise to a decrease of phase coherence between different sites, but they do not give rise to an immediate depopulation of a site. Equation 9 demonstrates this explicitly: $\hat{\Gamma}'\rho_{i,i} = 0$, whereas $\hat{\Gamma}'\rho_{i \neq j} = \Gamma$. Of course, when the pigments interact with each other, energy is transferred, but this transfer is not described by $\hat{\Gamma}'$ alone. The operator $\hat{\Gamma}'$ acts at the density matrix level; that is, it acts on $|i\rangle\langle j|$. In a matrix representation $\hat{\Gamma}'$ correspond to very large, $N^2 \times N^2$ matrix.

Rather than calculating the time evolution of the density matrix it turns out that it is better to calculate the Laplace transform of the density matrix,

$$\rho(z) = \int_0^\infty e^{-zt} \rho(t) \quad (10)$$

We will be interested only in the case $z = 0$. The formal solution of eq 8 is

$$\begin{aligned} \rho(z) &= (z - i\mathcal{L} + \hat{\Gamma}')^{-1} \rho(t=0) \\ &= G(z) \rho(t=0) \end{aligned} \quad (11)$$

where the Liouville operator \mathcal{L} is given by

$$-i\mathcal{L}\rho(t) = -iH\rho(t) + i\rho(t)H^* \quad (12)$$

Equation 11 is the defining relation for the Green function $G(z)$. To calculate $G(z)$ an $N^2 \times N^2$ matrix must be inverted. However, the problem can be simplified by using the very special form of the dephasing operator. We separate

$$\hat{\Gamma}' = \Gamma - \hat{\Gamma} \quad (13)$$

where Γ is a number operator identical to the Γ introduced above, and

$$\hat{\Gamma}|i\rangle\langle j| = \Gamma\delta_{ij}|i\rangle\langle j| \quad (14)$$

We next introduce the so-called noninteracting Green function G_0 , in which $\hat{\Gamma}$ is ignored:

$$G_0(z) = (z - i\zeta + \Gamma)^{-1} \quad (15)$$

G_0 can easily be calculated in terms of the eigenfunctions $|\psi_k\rangle$ and eigenvalues ω_k of H as

$$G_0(z)(|i\rangle\langle j|) = \sum_{k,k'} |\psi_k\rangle \frac{\langle\psi_k|i\rangle\langle j|\psi_{k'}^*\rangle}{z - i\omega_k + i\omega_{k'}^* + \Gamma} \langle\psi_{k'}^*| \quad (16)$$

As H is non-hermitian, we must make a distinction between left and right eigenfunctions. We now note that $\hat{\Gamma}$ is a very simple operator: it is diagonal in the $|i\rangle\langle j|$ basis, and more significantly, only N out of N^4 entries are nonzero. The only nonzero matrix elements are between density matrices of the form $|i\rangle\langle i|$. These matrix elements correspond to populations, as $\langle i|\rho(t)|i\rangle$ is the probability of finding molecule i excited. For the Green function we find

$$\begin{aligned} G(z) &= \frac{1}{z - i\zeta + \Gamma - \hat{\Gamma}} \\ &= \frac{1}{z - i\zeta + \Gamma} + \frac{1}{z - i\zeta + \Gamma} \hat{\Gamma} \frac{1}{z - i\zeta + \Gamma} + \\ &\quad \frac{1}{z - i\zeta + \Gamma} \hat{\Gamma} \frac{1}{z - i\zeta + \Gamma} \hat{\Gamma} \frac{1}{z - i\zeta + \Gamma} + \dots \\ &= G_0(z) + G_0(z) T(z) G_0(z) \end{aligned} \quad (17)$$

This equation defines the so-called **T**-matrix $T(z)$. While formally T is an $N^2 \times N^2$ matrix, it is clear from eq 17 that only matrix elements between populations are nonzero. Moreover, to find T only N^2 out of N^4 matrix elements of $G_0(z)$ are needed, as can be seen from eq 17. We find

$$\begin{aligned} T(z) &= \hat{\Gamma} + \hat{\Gamma} \frac{1}{z - i\zeta + \Gamma} \Gamma + \dots \\ &= \hat{\Gamma} \frac{1}{1 - G_0(z)\hat{\Gamma}} \end{aligned} \quad (18)$$

where the inverse is the inverse of an $N \times N$ matrix, the matrix elements of which are

$$[1 - G_0(z)\hat{\Gamma}]_{nn'} = \delta_{nn'} - [G_0(z)]_{nn'}\Gamma \quad (19)$$

Equation 18 represents an enormous improvement: we started with an $N^2 \times N^2$ problem, which is now simplified to an $N \times N$ problem through the use of Green functions. Equations 17 and 18 are the starting point for the calculations in this paper.

III. The Förster Transfer Limit

For the case where the homogeneous line width is much larger than the interaction ($\Gamma \gg J$), the interaction can be treated as a small perturbation and the energy transfer can be described as hopping of excitations.⁸ This we denote as the Förster limit as opposed to the exciton limit in which $J \gg \Gamma$. The general case we will denote as the mixed model. The relation with the solution derived in section II will now be elucidated. In the

hopping model the probabilities P_i of finding molecule i excited change in time according to

$$\begin{aligned} \frac{d}{dt}P_i &= \sum_j [W^{(F)}(i \leftarrow j)P_j - W^{(F)}(j \leftarrow i)P_i] \\ &\equiv \hat{W}P_j \end{aligned} \quad (20)$$

where the Förster transfer rates $W^{(F)}$ follow from a calculation of the spectral overlap integral.¹ As the homogeneous width is much larger than the interaction J and considering the high-temperature limit, pigment i has a Lorentzian absorption spectrum centered around ω_i and full width at half-maximum of Γ . The special pigment 1 is also lifetime broadened and has a full width at half-maximum of $\Gamma + \Gamma_d$. So the width of the absorption line of pigment i is given by

$$\Gamma_i = \Gamma + \Gamma_d \delta_{i,1} \quad (21)$$

The Förster transfer rates are given by

$$W^{(F)}(i \leftarrow j) = \frac{2J_{ij}^2}{\Gamma_{ij}} \left[1 + \left(\frac{\omega_i - \omega_j}{\Gamma_{ij}} \right)^2 \right]^{-1} \quad (22)$$

with $\Gamma_{ij} = (\Gamma_i + \Gamma_j)/2$. As we are considering the high-temperature case, $W^{(F)}(i \leftarrow j) = W^{(F)}(j \leftarrow i)$. To recover the r^{-6} dependence of the Förster energy transfer rate,¹ we note that for dipole-dipole interactions $J \propto r^{-3}$. The rates eq 22 are valid for $\Gamma \gg J$ irrespective of Γ_d . The Laplace transform of P_i , $P_i(z)$, is found as

$$P_i(z) = \frac{1}{z - \hat{W}^{(F)}} P_j(t=0) \quad (23)$$

where now only an $N \times N$ matrix must be inverted.

We have just described the hopping picture. We now show that identical results are obtained in the large Γ limit of the results of section II. For notational clarity we will ignore the distribution of frequencies for this argument, and put $\omega_i = 0$. Moreover we ignore the irreversible decay and put $\Gamma_d = 0$. In the limit $\Gamma \gg J$ we can find $G_0(z=0)$ perturbatively:

$$G_0(z=0) = \frac{1}{\Gamma} - \frac{1}{\Gamma^2}[H, \dots] + \frac{1}{\Gamma^3}[H, [H, \dots]] + \dots \quad (24)$$

The second term does not couple population matrix elements of the density matrix so that we do not require this term in the calculation of T . We thus find

$$\begin{aligned} [1 - G_0(z)\hat{\Gamma}]_{nn'} &= -\frac{1}{\Gamma^2}[H, [H, \dots]]_{nn'} \\ &= \frac{2J_{nn'}^2}{\Gamma^2} - \delta_{nn'} \sum_{n_1} \frac{2J_{nn_1}^2}{\Gamma^2} \\ &\equiv \frac{1}{\Gamma} W_{nn'}^{(x)} \end{aligned} \quad (25)$$

Note that the matrix elements of $\hat{W}^{(x)}$ are identical to the Förster matrix elements $\hat{W}^{(F)}$. The Green function becomes

$$G(z=0) = \frac{1}{\Gamma} + [W^{(x)}]^{-1} \quad (26)$$

The first term on the right-hand side corresponds to a coherent contribution that in the time domain corresponds to an exponentially decaying contribution, with a decay time $1/\Gamma$. We will ignore it in the remainder of this paper. The second term

is essentially eq 23. We thus have shown that the Green function approach of section II is a generalization of the Förster model and reduces to the hopping picture when $\Gamma \gg J$. For the general case of unequal ω_i , the rates eq 22 are found from a slightly more complicated calculation.

IV. Solution for a Ring

In the previous section we considered the case $\Gamma \gg J$. For typical situations occurring in photosynthesis this is not justified. In the Introduction we pointed out that a very reasonable estimate is $J/\Gamma = 2$. To study the consequences of this, we apply the Green function solution to a simple situation, that of an antenna complex in the form of a ring. While this is a reasonable assumption to make, we will also assume that the reaction center is included in the ring as one of the molecules. This model is taken for illustration purposes only, there is no known antenna structure with this geometry. We take the nearest neighbor interaction

$$J_{ij} = J\delta_{|i-j|,1} \quad (27)$$

and we assume periodic boundary conditions so that $J_{1,N} = J_{N,1} = J$. We will assume that initially all molecules are excited with equal probability and without phase coherence between different molecules. Then $\rho_{ij}(t=0) = \delta_{ij}/N$. We are interested in the average survival time of these excitations. There is no unique measure for the survival time. As is commonly done, we take the zeroth moment of $\rho(t)$:

$$t_s \equiv \int_0^\infty dt \rho_{n,n}(t) = \sum_n \rho_{n,n}(z=0) \quad (28)$$

For Förster transfer the survival time can be found using the methods of Pearlstein.^{11,12} In the present context the result can be written as

$$t_s = Nt_d + \frac{N^2 - 1}{12}t_h \quad (29)$$

with the decay time $t_d = 1/\Gamma_d$ and the hopping time

$$t_h = (2J/2\Gamma)^{-1} \quad (30)$$

Incidentally, for the parameters given $t_h = 5$ fs, which is a completely unrealistically short time, indicating that the energy transfer is not described by the Förster rates. The first term in eq 29 represents the average reaction time; the excitation will, on average, spend $1/N$ of its time on molecule 1, from where it can disappear from the system. The second term describes the time duration of energy transport. We have not found a closed result for the exciton model, but the calculation of the excitation lifetime is simple on a computer: computing the inverse of eq 18 is standard, and the excitation lifetime then follows from eq 28. There are three dimensionless parameters characterizing the problem: the number of pigments N , the ratio of the interaction and the homogeneous line width J/Γ , and the decay rate ratio Γ_d/Γ . In the presentation of the numerical results we have kept N and Γ_d/Γ constant. A typical result is presented in Figure 1. We find that the exact solution, the hopping approach, and eq 29 produce virtually identical results for this case, for which the excitation lifetime is mainly determined by the reaction rate.

These conclusions are modified only when we consider unrealistic parameters. In Figure 2 we have presented similar curves for the transport-limited situation in which $\Gamma_d = 10\Gamma$. For this value of the single-site annihilation rate, the special

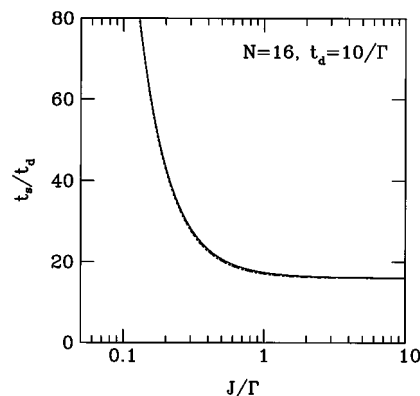


Figure 1. Dimensionless survival time t_s of a ring as a function of the ratio of nearest neighbor interaction J and homogeneous line width Γ . In this figure the single site decay rate $\Gamma_d = 1/t_d$ is fairly small, $\Gamma_d = \Gamma/10$. While barely visible, three almost identical curves are presented. The solid line is the exact result, the dashed line is the result of the hopping model, and the dotted line is the analytical result, eq 29. Clearly the analytical result is very accurate even when $J > \Gamma$. The reason for this is that whenever the interaction J is large so that the hopping picture is not valid, the lifetime is determined by the reaction time (the first term in eq 29).

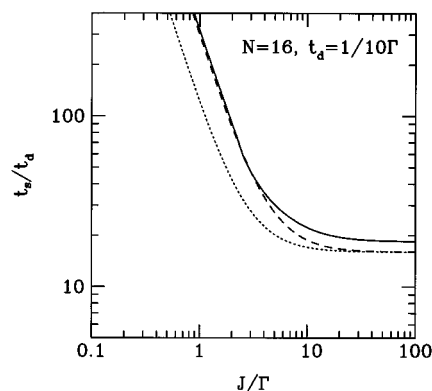


Figure 2. Survival time t_s in units of the single-site decay time as a function of the ratio of nearest neighbor interaction J and homogeneous line width Γ . As in Figure 1, the solid line is the exact result, the dashed line is the result of the hopping model, and the dotted line is the analytical result, eq 29. Now the decay rate is unrealistically large, $\Gamma_d = 10\Gamma$. Comparing the solid line to the dashed line, we find that only for quite large interaction strengths J does the hopping picture become inaccurate. Equation 29 is always inaccurate, as for this rapid decay rate the reaction center is lifetime broadened (eq 21) so that the Förster transfer rate to the reaction center is not equal to the other transfer rates, $W(1 \leftarrow 2) \neq W(i \leftarrow i+1)$.

molecule that models the reaction center is substantially lifetime broadened so that eq 29 is always inaccurate. The hopping picture gives somewhat inaccurate results only deep in the exciton regime, when $J > 5\Gamma$. We conclude that a major reason for the success of the Förster approach in photosynthesis is that whenever the hopping model fails to describe the dynamics correctly, the survival time is limited by the reaction rate, and the dynamics is irrelevant as far as the survival time is concerned. This observation holds even stronger for a physical antenna system coupled to a reaction center as the reaction center presumably is located in the middle of a ring of antenna complexes so that the most important energy transfer process is the transfer to the reaction center, not the energy transfer within the antenna.¹² An excitation lifetime study is insensitive to the effects of excitation coherence.

A situation that is of much more physical interest is when inhomogeneous broadening is present. This is incorporated by taking various individual molecule transition frequencies ω_i . Because of the inhomogeneous broadening, the dynamics of

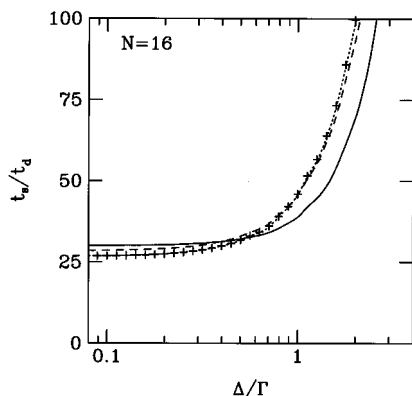


Figure 3. Dimensionless survival time t_s as a function of the ratio of inhomogeneous width Δ and homogeneous width Γ for a ring of 16 pigments where $\Gamma_d = \Gamma$. Dotted line: $\Gamma = 10J$. For this Γ there is no difference between the exciton calculation and the hopping result (indicated by +). Solid line: $\Gamma = J$, exciton calculation. Dashed line: $\Gamma = J$, hopping approximation. The hopping picture is slightly inaccurate when $\Gamma = J$, as then coherent effects such as superexchange are not taken into account.

the excitation is modified. In Figure 3 we present the result of simulations where the ω_i are randomly drawn from a Gaussian distribution with standard deviation Δ . When inhomogeneous broadening is significant and J is comparable to Γ , the hopping picture becomes somewhat inaccurate. This is due to the fact that hopping does not take into account coherent effects such as superexchange. Yet, as above, the difference between the exciton calculation and the hopping calculation is only minor.

V. Application to Light-Harvesting Complexes

Recently the structure of the light-harvesting complex 2 (LH2) of *Rhodospseudomonas acidophila* was solved.⁴ It was found that the B850 absorption is due to a ring of 18 pigments. Assuming that the fundamental spectroscopic unit is a dimer, we can relate this LH2 complex to our model for a ring of $N = 9$ dimers. Recently femtosecond experiments on LH1 of *Rhodobacter sphaeroides* with the reaction center removed were performed.¹³ While the structure of the LH1 complex is not known, it is assumed that it is a ring of $N = 16$ dimers. Other numbers are also assumed, for instance in ref 13 an interpretation of experimental results is presented assuming $N = 8$.

The two studies of ref 13 were fluorescence depolarization and singlet–singlet annihilation. The theoretical description of the singlet–singlet annihilation process is very similar to that of excitation decay described in the previous section. The most significant difference is that singlet–singlet annihilation supposedly takes place when the two excitations are next to each other. This can easily be incorporated in the model studied in this paper. Firstly the index now denotes the relative distance of the two excitations. Secondly we add the term $-i\Gamma_d|N\rangle\langle N|/2$ to the effective Hamiltonian of eq 1. The third modification is that we have to replace the periodic boundary condition by a reflecting boundary condition as the two excitations cannot cross each other. Effectively this amounts to putting $J_{1,N} = J_{N,1} = 0$. The singlet–singlet lifetime can then be calculated using the techniques of refs 11 and 12. We find

$$t_s = \frac{N}{2}t_d + \frac{(N-1)(N-2)}{12} \frac{t_h}{2} \quad (31)$$

Comparing this with eq 29, we note that the reaction time (the first term on the right-hand side) is halved, as there are now two reaction sites. Also the hopping time t_h is halved, as we are only interested in the relative distance of the two excitations.

Due to the reflecting boundary conditions, the prefactor to the transport term is somewhat different from that found in eq 29. For small rings the difference can be significant. We have not studied the effect of disorder on eq 31, as this is complicated by the fact that then not only the relative distance of the two excitations is important but also the location of the two excitations on the underlying structure is important.

While singlet–singlet annihilation is not very sensitive to the nature of the energy transfer mechanism, we now show that the depolarization time is sensitive to J/Γ . For a consistent interpretation the issue of exciton coherence cannot be ignored. The model studied in the previous section does not quite apply to LH1. We now suggest possible interpretations for these experiments within the context of the discussion of coherent versus incoherent energy transport. The extension of the theory to the depolarization experiment is simple. As there is no reaction site, we put $\Gamma_d = 0$. The pulse that is used to create the initial population of excitations is polarized. The direction of the transition dipoles of the pigments varies along the ring, so an anisotropic distribution of excitation is created. The excitation density is assumed to be given by

$$\rho_{n,n}(t=0) = \rho_0 + \rho_p \left[\cos^2\left(\frac{2\pi n}{N}\right) - \frac{1}{2} \right] \quad (32)$$

where ρ_p describes the amount of anisotropy. As the transition dipoles are oriented the fluorescence is polarized. The distribution will relax toward an isotropic distribution. Due to the orientation of the ring, the fluorescence will not decay to zero and a small residual anisotropic signal will remain. The part of the polarization that is decaying because of the energy transfer is proportional to

$$P(t) \propto \sum_n [\cos^2(2\pi n/N) - \sin^2(2\pi n/N)] \rho_{n,n}(t) \quad (33)$$

Similar to before, we can define a measure for the depolarization time as the zeroth moment of $P(t)$. This can be found in terms of the Green function of section II. Summing eq 33 and a similar contribution with a sine, we find a measure for the depolarization time:

$$t_{\text{dep}} = \frac{1}{N} \sum_{n,n'} \cos\left(\frac{4\pi}{N}(n-n')\right) G_{nn',n'n'}(z=0) \quad (34)$$

For a ring without disorder we can find an analytical result for the depolarization time. As we have put $\Gamma_d = 0$, the eigenfunctions of H are plane waves. Hence G_0 can be obtained in closed form.¹⁰ As the ring is isotropic, $G_{0,nn'}$ only depends on $n - n'$ so that also T can be calculated. We finally find

$$t_{\text{dep}} = \frac{1}{\Gamma} \frac{1}{1 - G_0 T} \quad (35)$$

with

$$G_0 T = \frac{1}{N} \sum_{k=1}^N \frac{\Gamma^2}{\Gamma^2 + 16J^2 \sin^2(2\pi/N) \sin^2(2\pi k/N)} \quad (36)$$

For large N the sum can be replaced by an integral, resulting in

$$G_0 T = \left\{ 1 + \left[\frac{4J}{\Gamma} \sin\left(\frac{2\pi}{N}\right) \right]^2 \right\}^{-1/2} \quad (37)$$

For small interaction J the depolarization time becomes

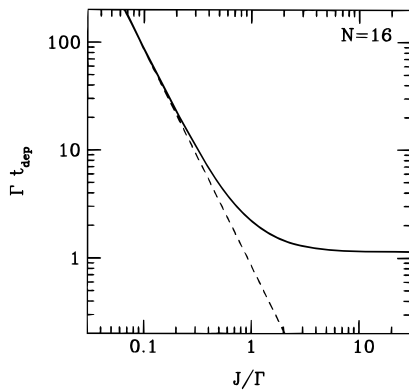


Figure 4. Depolarization time t_{dep} multiplied by the dephasing rate Γ as a function of the scaled nearest neighbor coupling J/Γ for a ring of $N = 16$ pigments. Solid line: exact result. Dashed line: Förster limit. The hopping result $t_{\text{dep}}\Gamma = \Gamma^2/4J^2 \sin^2(2\pi/N)$ holds for $J \ll \Gamma$. The hopping picture fails when $t_{\text{dep}} \approx 1/\Gamma$. The physical reason for this is that in order to have a depolarization, there must be decay, and the decay rate is essentially Γ . In contrast to the fluorescence lifetime, the depolarization is sensitive to the excitonic nature of the energy transport.

$$t_{\text{dep}} = \frac{t_h}{4 \sin^2(2\pi/N)} \quad (38)$$

as was found before by ref 13. The significance of eq 37 is that it explicitly shows when a crossover behavior from hopping dynamics to exciton dynamics is to be expected. For reasonable estimates of the parameters appropriate for LH1 we find that we are indeed in the crossover regime and eq 38 is inaccurate. In Figure 4 we graphed prediction eq 35. For a ring with a significant amount of disorder the effect of coherence is reduced. This is illustrated in Figure 5.

In ref 13 the fluorescence depolarization was found to decay on a time scale on the order of 200 fs. They interpreted their experiments assuming a ring of $N = 16$ pigments, an interaction energy $J = 250 \text{ cm}^{-1}$, a homogeneous broadening of $\Gamma = 250 \text{ cm}^{-1}$, and an inhomogeneous broadening of $\Delta = 250 \text{ cm}^{-1}$. Using the theory described here, we obtain $t_{\text{dep}} \approx 60 \text{ fs}$, which is much too fast. If we assume that Γ and Δ are correct, we find that $t_{\text{dep}} \approx 200 \text{ fs}$ for $J = 80 \text{ cm}^{-1}$. The singlet–singlet annihilation time of LH1 of *R. sphaeroides* was found to be about 1 ps. However using the given parameters with interaction energy $J = 80 \text{ cm}^{-1}$, we find a singlet–singlet annihilation rate of $t_s > 3 \text{ ps}$, which is incompatible with experimental results. We have not found a set of parameters that offers a consistent interpretation of the experimental results of ref 13.

VI. Discussion

In this paper we have shown how the Green function formalism can be applied to photosynthetic antenna systems. We have shown that the lifetime of an excitation does not depend sensitively on the excitonicity of the energy transfer. Only for primarily inhomogeneously broadened antenna systems (large disorder) can differences between coherent and hopping dynamics be found. The situation is almost the opposite for the depolarization time. The predicted depolarization time is dependent on the nature of the exciton dynamics. Whenever the ratio of interaction strength over homogeneous line width J/Γ is on the order of unity, significant deviations from hopping dynamics are predicted. A reasonable estimate is $J/\Gamma = 2$; this will be significant in the interpretation of experimental results. As far as LH1 is concerned, other interpretations of the experimental results are possible. The point of view of ref 13 is that the finite temperature combined with static disorder can

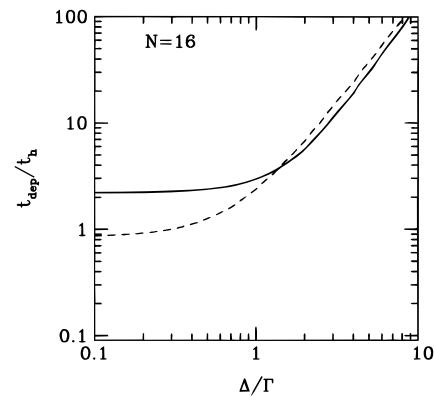


Figure 5. Depolarization time t_s divided by the Förster hopping time $t_h = \Gamma/2J^2$ as a function of the ratio of disorder Δ divided by the homogeneous line width Γ . In this figure results for a ring of $N = 16$ pigments are presented and $\Gamma = J$. The dashed curve is the result of the diffusion approximation, and the solid curve the exact exciton result. Disorder reduces the effect of coherent exciton dynamics.

be used to provide a consistent interpretation of the spectroscopic data. Nevertheless, as soon as the interaction strength becomes comparable to the homogeneous line width, coherent effects cannot be ignored.

In discussing the exciton dynamics it would be useful to have a number that indicates the average “size” of an excitation, or rather, the number of coherent pigments. Here we propose a simple extension of the concepts used in the theory of localization.^{14,15} We define the generalized average participation ratio:

$$R = \sum_i \Gamma G_{ii,ii}^{(0)}(z=0) \quad (39)$$

This is the time-integrated probability that an excitation that started at site i can be found at the same site, weighted by the dephasing time.^{14,15} In terms of the eigenfunctions $|\psi_k\rangle$ with energies ω_k , the generalized participation ratio is given by

$$R = \frac{\Gamma}{N_{i,k,k'}} \sum_{i,k,k'} \int_0^\infty dt e^{-\Gamma t} e^{i(\omega_k - \omega_{k'})t} |\langle i|\psi_k\rangle|^2 |\langle i|\psi_{k'}\rangle|^2 \\ = \frac{1}{N_{i,k,k'}} \sum_{i,k,k'} |\langle i|\psi_k\rangle|^2 \frac{\Gamma^2}{\Gamma^2 + (\omega_k - \omega_{k'})^2} |\langle i|\psi_{k'}\rangle|^2 \quad (40)$$

In the limit of zero homogeneous line width $\Gamma \rightarrow 0$, R tends to the usual participation ratio:

$$R(\Gamma=0) = \frac{1}{N_{i,k}} \sum_{i,k} |\langle i|\psi_k\rangle|^4 \quad (41)$$

which is valid when there are no degenerate states. The inverse participation ratio,

$$N_{\text{coh}} = 1/R \quad (42)$$

is universally taken as the number of coherent molecules,^{14,15,16} valid when there is no homogeneous broadening.

In the Förster limit of very large Γ the exciton dynamics is incoherent, which can also be interpreted as a hopping excitation. In this case only one molecule is excited at the time. A very attractive property of the generalized participation ratio R is that it does just that; it can easily be shown that in the limit of $\Gamma \rightarrow \infty$, $R = 1$. The inverse generalized participation ratio $1/R$ is a good measure for the number of coherent molecules. A desirable property of R is that it is a physical quantity, as it is

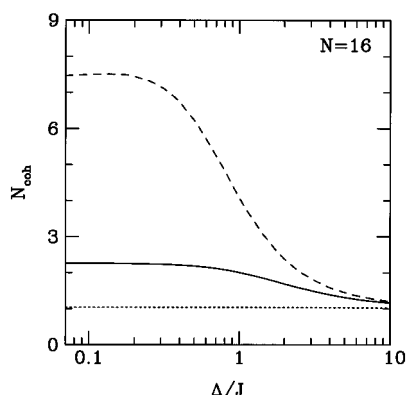


Figure 6. Inverse generalized participation ratio $1/R = N_{\text{coh}}$ as a function of disorder Δ divided by the interaction energy J for a linear periodic chain of $N = 16$ molecules. Solid line: $\Gamma = J$. Dashed line: $\Gamma = J/10$. Dotted line: $\Gamma = 10J$. For large homogeneous line widths the number of coherent molecules is 1, irrespective of the amount of disorder. For small homogeneous line widths the number of coherent molecules decreases with increasing disorder, which is the onset of the usual localization behavior.

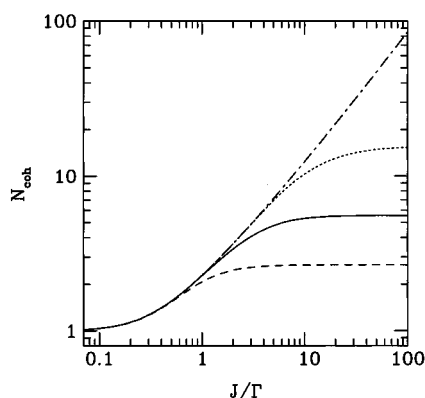


Figure 7. Inverse generalized participation ratio $1/R = N_{\text{coh}}$ as a function of the interaction energy J divided by the homogeneous line width Γ for a linear periodic chain without disorder. Dashed line: $N = 4$. Solid line: $N = 10$. Dotted line: $N = 30$. The dot-dashed line represents the infinite size limit, eq 44. For a realistic value of $J = 2\Gamma$ only about four molecules are coherent, even for large complexes. The number of coherent molecules does not tend to N in the exciton limit (J large) because of the degeneracy of the ring.

a certain moment of the Green function. This means that it is independent of the basis set used, for example. In Figure 6 we present results for the number of coherent molecules as a function of the amount of inhomogeneous broadening. We find that N_{coh} satisfies the expected limiting cases. Because of the degeneracy in the absence of disorder, $N_{\text{coh}} < N$ even at $\Delta = 0$.

Without disorder, explicit results for R can be obtained:

$$R = \frac{1}{N} \sum_{k_1, k_2=1}^N \frac{\Gamma}{\Gamma + 2iJ \cos \frac{2\pi k_1}{N} - 2iJ \cos \frac{2\pi k_2}{N}} \quad (43)$$

The resulting coherence sizes are presented in Figure 7. We find that for sufficiently large systems N_{coh} converges. For large N the sum in eq 43 can be replaced by an integral, resulting in¹⁴

$$R = \frac{2}{\pi} K\left(i \frac{4J}{\Gamma}\right) \quad (44)$$

where K is the complete elliptic integral of the first kind.¹⁴ This

function is used to obtain the dot-dashed line in Figure 7. In the large interaction limit we obtain

$$N_{\text{coh}} = \frac{2\pi J}{\Gamma \log(J/\Gamma)} \quad (45)$$

For LH1 Bradforth *et al.* found that $J = \Gamma$ and $\Delta = \Gamma$, and we assume that $N = 16$. For these values we find that $N_{\text{coh}} = 2.03$. Without disorder we find $N_{\text{coh}} = 2.07$, and ignoring the phonons gives $N_{\text{coh}} = 4.85$. We conclude that for LH1 of *R. sphaeroides* the excitation is delocalized over about two dimers. Moreover, the localization is due to the phonons and not due to the static disorder.

It remains to be seen to what extent the average number of coherent molecules corresponds to an experimentally observable quantity. The number presented in this paper follows from an admittedly indirect approach: a theoretical calculation based on parameters that are obtained by combining the presumed structure of LH1 with the experimental results for the fluorescence depolarization. Recently¹⁷ pump-probe experiments on J-aggregates were related to an exciton size. However, the theory used in ref 17 did not take into account the homogeneous dephasing caused by phonons, so that it is unlikely that it can be applied to photosynthetic systems. The calculation of pump-probe spectra (or photon echo) from an approach as used in this paper is the route to go. It is also quite complicated as, at least in the straightforward approach, the density matrix becomes an $N^2 \times N^2$ matrix.

Acknowledgment. This research has been made possible by a fellowship of the Royal Netherlands Academy of Arts and Sciences (KNAW). I thank Dr. F. van Mourik for many valuable discussions.

References and Notes

- (1) Förster, Th. In *Modern Quantum Chemistry*; Sinannoglu, O., Ed.; Academic Press: New York, 1965; p 93.
- (2) Matthews, B. W.; Fenna, R. E.; Bolognesi, M. C.; Schmid, M. F.; Olsen, J. M. *J. Mol. Biol.* **1979**, *131*, 259. Pearlstein, R. M. *Photosynth. Res.* **1992**, *31*, 213.
- (3) Mukamel, S. *Principles of Nonlinear Optical Spectroscopy*; Oxford: New York, 1995.
- (4) McDermott, G.; Prince, S. M.; Freer, A. A.; Hawthornthwaite-Lawless, A. M.; Papiz, M. Z.; Cogdell, R. G.; Isaacs, N. W. *Nature* **1995**, *374*, 517.
- (5) Sauer, K.; Scheer, H. *Biochim. Biophys. Acta* **1988**, *936*, 157.
- (6) MacColl, R.; Csatorday, D.; Berns, S.; Traeger, E. *Biochemistry* **1980**, *19*, 2817.
- (7) Durrant, J. R.; Klug, D. R.; Kwa, S. L.; Van Grondelle, R.; Porter, G.; Dekker, J. P. *Proc. Natl. Acad. Sci. U.S.A.* **1995**, *92*, 4798.
- (8) Kenkre, V. M. In *Exciton Dynamics in Molecular Crystals and Aggregates*; Springer: Berlin, 1982. See also the article by P. Reineker in this book.
- (9) Wannier, G. *Elements of Solid State Theory*; Cambridge: Cambridge, 1959.
- (10) Haken, H.; Strobl, G. *Z. Phys.* **1973**, *262*, 135.
- (11) Pearlstein, R. M. *Photochem. Photobiol.* **1982**, *35*, 835.
- (12) Somsen, O. J. G.; Van Mourik, F.; Van Grondelle, R.; Valkunas, L. *Biophys. J.* **1994**, *66*, 1580.
- (13) Bradforth S. E.; Jimenez, R.; Van Mourik, F.; Van Grondelle, R.; Fleming, G. R. *J. Phys. Chem.* **1995**, *99*, 16179.
- (14) Economou, E. N. *Green's Functions in Quantum Physics*; Springer: Berlin, 1979.
- (15) Thouless, D. J. *Phys. Rep.* **1974**, *13C*, 94.
- (16) Fidler, H.; Knoester, J.; Wiersma, D. A. *J. Chem. Phys.* **1991**, *95*, 7880.
- (17) Van Burgel, M.; Wiersma, D. A.; Duppen, K. *J. Chem. Phys.* **1995**, *102*, 20.